Volume Changes Correlate with Enthalpy Changes during the Photoinduced Formation of the ^{3}MLCT State of Ruthenium(II) Bipyridine Cyano Complexes in the Presence of Salts. A Case of the Entropy−Enthalpy Compensation Effect†

Claudio D. Borsarelli and Silvia E. Braslavsky*

Max-Planck-Institut für Strahlenchemie, Postfach 10 13 65, D-45413 Mülheim an der Ruhr, Germany

Received: February 22, 1998; In Final Form: May 18, 1998

The total structural volume (ΔV_{str}) and enthalpy (ΔH_{str}) changes associated with the formation of the triplet metal-to-ligand charge transfer (^{3}MLCT) state were determined by laser-induced optoacoustic spectroscopy for the complexes $Ru(bpy)_3^{2+}$, $Ru(bpy)_2(CN)_2$, and $Ru(bpy)(CN)_4^{2-}$ in aqueous solutions of 0.1 M monovalent salts. For the cyano complexes (bound to water through hydrogen bonds) the values of ΔV_{str} vs ΔH_{str} exhibited a linear relationship in the salt series, whereas for $Ru(bpy)_3^{2+}$ the values were independent of the salt. This linear correlation is interpreted as arising from an enthalpy−entropy compensation effect of the water structure perturbed by the 0.1 M salts. Since in all cases the intrinsic energy of the ^{3}MLCT state was unperturbed by the salts (as determined by the constancy of the absorption and emission spectra), the plots ΔH_{str} vs ΔV_{str} (the latter shown to be proportional to ΔS_{str}) yield the free energy for the formation of the ^{3}MLCT state, ΔG_{MLCT} = (123 ± 8) kJ/mol for $Ru(bpy)_2(CN)_2$ and (67 ± 25) kJ/mol for $Ru(bpy)(CN)_4^{2-}$. The higher stability of the ^{3}MLCT state of $Ru(bpy)(CN)_4^{2-}$ is due to the larger entropic factor which originates in the high flexibility photoinduced in its ^{3}MLCT state by the loosening of four CN-bound water molecules, rather than only two in $Ru(bpy)_2(CN)_2$. The correlation ΔV_{str} vs ΔS_{str} (a consequence of the correlation between the environment reorganization parameters ΔV_{sol} and ΔS_{sol}) finds support in the proportionality between ΔV_{str} of the cyano complexes and the calculated water-structuring entropy of the salts, $\Delta S°_{str}$(salt). Water structuring salts [negative $\Delta S°_{str}$(salt) values] afforded a larger ΔV_{str}, due to the extension of the water network, opposite to structure breaking salts [positive $\Delta S°_{str}$(salt) values] which yielded smaller ΔV_{str} values. For $Ru(bpy)(CN)_4^{2-}$ the linear dependence had twice as large a slope as for $Ru(bpy)_2(CN)_2$, reflecting the difference in the number of hydrogen-bound CN groups.

Introduction

The structural volume changes, ΔV_{str}, associated with the formation and decay of the triplet metal-to-ligand charge transfer (^{3}MLCT) state of several Ru(II) bipyridine cyano complexes in aqueous solution, determined by using laser-induced opto-acoustic spectroscopy (LIOAS), were attributed to photoinduced changes in the hydrogen bond strength between the cyano ligands and the water molecules in the first solvation shell.[1] The expansions found for the formation of the ^{3}MLCT state of the cyano and methyl isocyanide complexes, $Ru(bpy)(CN)_4^{2-}$, $Ru(bpy)(CN)_3(CNCH_3)^-$, $Ru(bpy)_2(CN)_2$, and $Ru(bpy)(CN)_2(CNCH_3)_2$, (ΔV_{str} ca. 15, 10, 5, and 0 cm^3/mol, respectively), correlated relatively well with the number of cyanide ligands available for hydrogen bond interactions with water. The expansions indicate that for these compounds the hydrogen bond interactions with water are weaker in the excited state than in the ground state.[1]

More recently, we have shown that when $Ru(bpy)(CN)_4^{2-}$ is dissolved into the water pools of reverse micelles of the anionic surfactant sodium bis(2-ethylhexyl)sulfosuccinate (AOT) in *n*-alkanes at 25 °C, the value of ΔV_{str}, the emission quantum yield, and the lifetime of the complex depend on the amount of water present in the water pool. For a high water content the behavior is like in homogeneous water solution, while for a low water content the rigidity of the water core is reflected in a much smaller expansion and somewhat higher emission lifetime and quantum yield.[2]

Our conclusions about the role of the water hydrogen bonds with the cyano ligands were in line with a variety of experimental data indicating a high sensitivity to the solvent[3−5] and to the pH[6] of the photophysical properties of mixed metal cyano pyridyl complexes. Moreover, correlations have been established between several properties associated with the ^{3}MLCT state of mixed Ru(II) cyano complexes (e.g., energy of absorption and emission bands and redox potentials), the acceptor number of the solvent, and the number of cyano ligands present in the complex.[4] The nature of the interaction is clearly explained by the Lewis-base character of the cyano ligands which donate the electron pair to individual solvent molecules.[7] In several publications it has been realized that those donor−acceptor interactions in the cyano complexes are stronger in the ground state than in the excited state.[4,6,8]

Taking into account the role played by the hydrogen bond in the aqueous solutions of Ru(II) bipyridine cyano complexes, these should be sensitive to changes in the properties of water induced by the addition of chaotropic and organizing agents such as salts, since these agents modify the extended three-dimensional network of hydrogen bonds in water.

In this paper we report on the effect of the addition of monovalent salts on the structural heat and volume changes

* Correspondence author. Fax: +49 208 306 3951. E-mail: braslavskys@mpi-muelheim.mpg.de.

† Abbreviations: bpy, 2,2′-bipyridine ligand; MLCT, metal-to-ligand charge-transfer complex; LIOAS, laser-induced optoacoustic spectroscopy.

S1089-5647(98)01235-8 CCC: $15.00
Published on Web 07/17/1998

associated with the formation and decay of the ^{3}MLCT state of $Ru(bpy)_3^{2+}$, $Ru(bpy)_2(CN)_2$, and $Ru(bpy)(CN)_4^{2-}$ in aqueous solutions, as determined by using LIOAS measurements. For the cyano complexes a correlation is found between the structural volume changes and, on one side, the heat produced during the formation of the ^{3}MLCT state and, on the other side, the water-structuring entropy of the salt.

These data are interpreted in terms of an enthalpy−entropy compensation effect along the salt series. This effect, especially evident in aqueous media, in dilute solutions is due to perturbations in thermodynamic quantities describing environmental effects.[9] Such a perturbation is produced, e.g., by the addition of hydrogen-bonding solutes to an aqueous solution in which hydrogen-bonding equilibria are established between various molecular species. In the case analyzed in this report the various molecular species change their equilibrium concentration as a consequence of the more or less organized water network induced by the added salt. The changes are sensed by the structural heat and the structural volume change (proportional to the entropy change) observed during the formation and decay of the ^{3}MLCT state of the cyano complexes.

Experimental Section

Materials and Solutions. $Ru(bpy)_3Cl_2 \cdot 6H_2O$ (bpy = 2,2′-bipyridine) was obtained from Aldrich. $Ru(bpy)_2(CN)_2$ and $Ru(bpy)(CN)_4K_2$ were supplied by Professor Franco Scandola (Ferrara, Italy). The calorimetric reference compounds $Ni(ClO_4)_2$, $Na_2Cr_2O_7$, bromocresol purple (BCP), and all the salts were obtained from Aldrich or Fluka in the highest purity available and used as received. Water was deionized. The concentration of the ruthenium complexes was ca. 5×10^{-5} M. In all cases the experiments were performed in 0.1 M salt solutions. With the $Ru(bpy)(CN)_4^{2-}$ complex, measurements were also performed in dispersions of reverse micelles prepared with sodium bis(2-ethylhexyl)sulfosuccinate (AOT, Sigma) in *n*-heptane (Merck) and containing the respective 0.1 M salt solution in its water pool. AOT dispersions were used in order to expand the range of the thermoelastic parameters in the LIOAS experiments.[2] The AOT concentration was 0.1 M, while the molar ratio water to surfactant was $R = [H_2O]/[AOT] = 20$. Under these conditions, the number of molecules of complex per micelle was < 0.1.

Methods. The absorbances of reference and sample solutions were recorded with a Shimadzu UV-2102PC spectrophotometer and matched within 3% at the laser excitation wavelength. The LIOAS setup has already been described.[1,10] Basically, for the $Ru(bpy)(CN)_4^{2-}$ complex, the LIOAS studies were performed using as the excitation pulse a 15 ns (fwhm) laser pulse at 400 nm produced by an Excimer laser (FL2000 Lambda Physik, XeCl)-pumped dye laser (EMG 101 MSC with the dye Furan 2, Lambda Physik). For the case of $Ru(bpy)_3^{2+}$ and $Ru(bpy)_2(CN)_2$, excitation was at 441 nm from the Excimer laser-pumped Coumarin 120 dye (Lambda Physik). A 40 μm poly(vinylidene fluoride) film was used as acoustic detector. The signals were amplified 100 times (Comlinear E103) and fed into a transient recorder (Tektronix TDS 684A, operating at 1 G sample/s and averaging 200/300 signals). The beamwidth was shaped with a slit (0.2 × 6) mm which determined an acoustic transit time of 120 ns, allowing transient detection down to ca. 15 ns by using deconvolution techniques.[2] The solutions were deoxygenated by Ar-bubbling for 10−15 min with solvent-saturated Ar. Temperature-dependent measurements were performed in the range 15.0−40.0 (±0.1) °C. The measurements with $Ru(bpy)(CN)_4^{2-}$ in AOT micelles were performed at 25.0 ± 0.1 °C. To avoid multiphotonic processes, the laser-pulse fluence was in every case smaller than 30 μJ, since even up to 50 μJ good linear dependency of the LIOAS signal amplitude with the laser fluence was observed. No photobleaching of the sample or the reference solutions was detected after each experiment.

Steady-state emission spectra were performed with a Spex Fluorolog spectrofluorometer in deoxygenated solutions at room temperature. Fluorescence lifetimes were determined with a single photon counting setup decribed elsewhere.[11]

LIOAS Signal Handling. The LIOAS signal handling using deconvolution was as reported in several previous publications.[1,2,10] A sum of two single-exponential decays fitting function was used for the time-resolved pressure evolution in the medium upon excitation of the sample. The recovered amplitudes (φ_i) of the fitting function, normalized with respect to the amplitude of the LIOAS signal for the calorimetric reference, are given by eq 1, where $\beta = (\partial V/\partial T)_P(1/V)$ is the

$$E_\lambda \varphi_i = q_i + \Delta V_i(c_p\rho/\beta) \tag{1}$$

cubic expansion coefficient, c_p is the heat capacity at constant pressure, ρ is the mass density of the medium, E_λ is the excitation energy per exciting Einstein (299.3 kJ/mol at 400 nm and 271.5 kJ/mol at 441 nm), q_i is the heat released in the particular relaxation process *i*, and ΔV_i ($=\Phi_i \Delta V_{str,i}$, with Φ_i the quantum yield and $\Delta V_{str,i}$ the structural volume change per mole of phototransformed species in the *i*th process) is the total contribution of the structural volume change to the signal.

The Sound Analysis version 1.13 software (Quantum Northwest) was used for deconvolution signal analysis. The amplitudes and lifetimes were obtained by averaging from two or three independent sets of measurements at three different fluence values for each solution. This procedure yields errors lower than 5 and 10% for the LIOAS amplitudes and decay times, respectively. The lifetimes present more scattering probably due to some variation in the deoxygenation procedure of the solutions. For the same sample, independent sets of data obtained with different calorimetric references yielded coincident results, within 5%. For the calorimetric reference BCP, the pH of the solutions was adjusted at 4 by adding small amounts of concentrated HCl, to use the yellow form of the dye.

Since aqueous solutions containing added salts have thermoelastic parameters different from those for neat water, the determination of the ratio $(c_p\rho/\beta)_T$ in the aqueous solutions at different temperatures was performed by comparing the fluence-normalized LIOAS signal amplitude for the calorimetric reference in water ($H_n^{r,w}$ with that in salt solutions ($H_n^{r,salt}$). Both signal amplitudes are related by the simple eq 2 already described.[2,12]

$$\frac{H_n^{r,w}(T)}{H_n^{r,salt}(T)} = \frac{(\beta/c_p\rho)T^w(\kappa_T)_T^{salt}}{(\beta/c_p\rho)_T^{salt}(\kappa_T)_T^{w}} \tag{2}$$

In aqueous solutions the isothermal compressibility, k_T, is almost identical to the adiabatic compressibility, k_S, i.e., $k_T = k_S = 1/(\rho v_a^2)$. The differences in the values of k_S for the solutions of the different salts were <3%, as calculated from the variation in the values of ρ for 0.1 M salt solutions with respect to the value of water[13] and the values of v_a determined from the variation of the arrival time of the acoustic wave to the detector.

Thus, the ratio of LIOAS signal amplitudes (left side in eq 2) affords the $(c_p\rho/\beta)_T$ salt values for 0.1 M salt solution. They

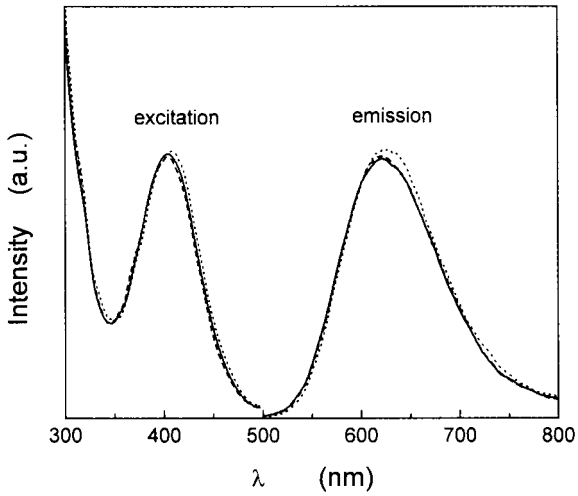

Figure 1. Emission and excitation spectra of $Ru(bpy)(CN)_4^{2-}$ with different salts: (•••) 0.1 M $N(CH)_4Cl$, $A_{400} = 0.207$; (- - -) 0.1 M CsCl, $A_{400} = 0.204$; (—) water, $A_{400} = 0.205$. λ_{exc}: 400 nm. λ_{em}: 620 nm.

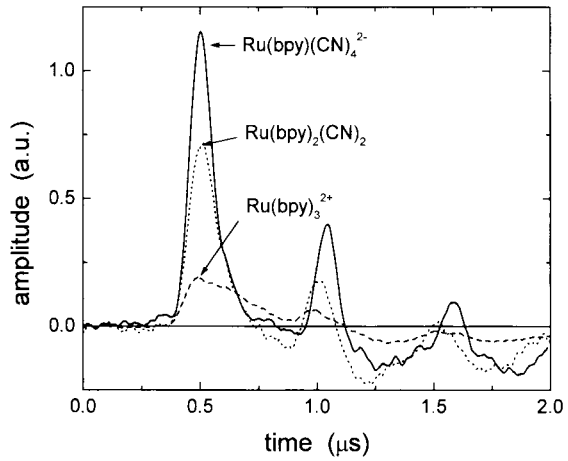

Figure 2. LIOAS signals for $Ru(bpy)_3^{2+}$, $Ru(bpy)_2(CN)_2$, and $Ru(bpy)(CN)_4^{2-}$ in 0.1 M NaBr aqueous solutions at 20 °C with laser excitation at 400 nm for $Ru(bpy)(CN)_4^{2-}$ and at 441 nm for $Ru(bpy)_3^{2+}$ and $Ru(bpy)_2(CN)_2$. Sample absorbance was at λ_{exc} ca. 0.25 in each case.

were 24.9, 22.4, 19.2, 15.5, 13.3, and 10.6 kJ/cm^3 (±5%) for 15, 17, 20, 25, 30, and 40 °C, respectively, and independent of the nature of the salt. For AOT/*n*-heptane/$R = 20$ dispersions at 25 °C the value estimated for $(c_p\rho/\beta)_T$ was (1.5 ± 0.1) kJ/cm.[32]

Results

The absorption, excitation, and emission spectra of the $Ru(bpy)_3^{2+}$, $Ru(bpy)_2(CN)_2$, and $Ru(bpy)(CN)_4^{2-}$ complexes in 0.1 M salt solutions were always the same as those in water.[4,8,14] As an example, typical emission and excitation spectra of $Ru(bpy)(CN)_4^{2-}$ in water and salt solutions are presented in Figure 1. The areas under the emission curves were identical for solutions of the same complex (identical absorbance) in neat water and in the presence of salts.

The emission lifetimes at 25 °C in salt solutions (640 ± 5) ns for $Ru(bpy)_3^{2+}$, (260 ± 2) ns for $Ru(bpy)_2(CN)_2$, and (101 ± 2) ns for $Ru(bpy)(CN)_4^{2-}$ were coincident with the values reported in water (650, 255, and 101 ns, respectively,[14]).

The LIOAS signals shown in Figure 2 were obtained for $Ru(bpy)_3^{2+}$, $Ru(bpy)_2(CN)_2$, and $Ru(bpy)(CN)_4^{2-}$ in 0.1 M NaBr, at 20 °C, and the same laser fluence, slit, and sample absorbance.

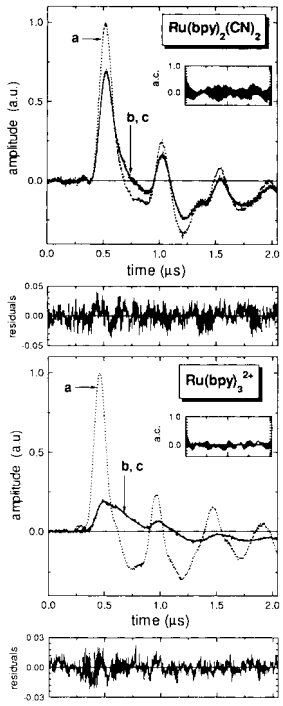

Figure 3. LIOAS signals for the reference $Na_2Cr_2O_7$ (curves a) and for $Ru(bpy)_2(CN)_2$ and $Ru(bpy)_3^{2+}$ (curves b) in 0.1 M CsCl solutions at 25 °C, together with the fits (curves c), residuals, and autocorrelation waveforms, after deconvolution using a sum of two single-exponentials decay function. Fitting results: $Ru(bpy)_2(CN)_2$, $\varphi_1 = 0.61$, $\tau_1 = 1$ ns, $\varphi_2 = 0.38$, $\tau_2 = 253$ ns, $\chi^2 = 1.66 \times 10^{-4}$; $Ru(bpy)_3^{2+}$, $\varphi_1 = 0.07$, $\tau_1 = 1$ ns, $\varphi_2 = 0.95$, $\tau_2 = 631$ ns, $\chi^2 = 4.06 \times 10^{-5}$. Note that the fitted curve completely coincides with the measured signal for the sample.

The shape of the signal depends on the complex. For a complex with a longer ^{3}MLCT lifetime, the LIOAS signal becomes broader and its amplitude decreases.

Satisfactory fits were obtained by deconvolution of the sample signal using a sum of two single-exponential decay functions in each case, as depicted in Figure 3 for $Ru(bpy)_2(CN)_2$ and for $Ru(bpy)_3^{2+}$ in 0.1 M CsCl in water. If all four parameters (two lifetimes and two preexponential factors) were allowed to freely vary, two well-separated components were obtained: (i) a fast component with a decay time $\tau_1 < 5$ ns in all cases; (ii) a slower component with a lifetime τ_2 between ca. 100 and 650 ns, depending on the complex.

The value of τ_1 was more or less arbitrary. This decay was faster than the time resolution of the LIOAS experiment. Fixing this parameter at any value between 1 ps and 5 ns always resulted in a similar value of the associated amplitude. The first component can thus be considered a reliable measure of all "prompt" processes, i.e., up to the ^{3}MLCT state formation.

The amplitude factors φ_1 and φ_2 at several temperatures were plotted as $E_\lambda\varphi_1$ and $E_\lambda\varphi_2$ vs $(c_p\rho/\beta)$, following eq 1. In all cases, good linear correlations were determined as shown in Figure 4 for $Ru(bpy)(CN)_4^{2-}$ in 0.1 M CsCl and in $N(CH_3)_4Cl$ solutions. The intercepts of the lines, q_1 and q_2 (Table 1), represent the heat released in the fast and in the slow process, respectively, i.e., during formation and decay of the ^{3}MLCT state of the complexes, and are interpreted using the energy balance eq 3,

$$E_\lambda - (q_1 + q_2 + \Phi_{em}E_{em}) = 0 \qquad (3)$$

where $\Phi_{em}E_{em}$ is the amount of energy (emission quantum yield times energy level of emitting state) lost by light emission which for the three complexes in aqueous solutions at room temperature is less than 8 kJ/mol, representing < 3% of E_λ.[1] Therefore,

TABLE 1: Heat Released, q_1 and q_2, and Volume Changes, ΔV_1 and ΔV_2, Associated with the Fast and the Slow Components in the LIOAS Signals for $Ru(bpy)_3^{2+}$, $Ru(bpy)_2(CN)_2$, and $Ru(bpy)(CN)_4^{2-}$ Complexes in Several Aqueous 0.1 M Salt Solutions

	$Ru(bpy)_3^{2+}$				$Ru(bpy)_2(CN)_2$				$Ru(bpy)(CN)_42-$			
salt	q_1 (kJ/mol)	q_2 (kJ/mol)	ΔV_1 (cm^3/mol)	ΔV_2 (cm^3/mol)	q_1 (kJ/mol)	q_2 (kJ/mol)	ΔV_1 (cm^3/mol)	ΔV_2 (cm^3/mol)	q_1 (kJ/mol)	q_2 (kJ/mol)	ΔV_1 (cm^3/mol)	ΔV_2 (cm^3/mol)
1. $N(CH_3)_4Cl$	81 ± 5	191 ± 8	-3.3 ± 0.4	3.5 ± 0.3	76 ± 7	193 ± 5	6.0 ± 0.4	-6.2 ± 0.3	59 ± 4	260 ± 6	18.2 ± 0.4	-19.2 ± 0.3
2. NH_4Cl	79 ± 5	194 ± 7	-3.6 ± 0.4	3.4 ± 0.4	86 ± 9	185 ± 6	5.1 ± 0.3	-4.9 ± 0.3	73 ± 4	232 ± 6	15.6 ± 0.2	-15.8 ± 0.3
3. KCl	77 ± 4	190 ± 8	-3.5 ± 0.3	3.2 ± 0.2	89 ± 7	183 ± 7	4.7 ± 0.4	-5.0 ± 0.2	70 ± 5	234 ± 5	15.5 ± 0.2	-15.7 ± 0.2
4. CsCl	73 ± 4	196 ± 7	-3.6 ± 0.2	3.4 ± 0.4	98 ± 5	166 ± 4	4.0 ± 0.3	-4.1 ± 0.1	84 ± 3	215 ± 4	13.7 ± 0.2	-14.1 ± 0.2
5. NaCl	79 ± 9	194 ± 9	-3.5 ± 0.2	3.7 ± 0.3	73 ± 6	192 ± 4	5.7 ± 0.3	-5.6 ± 0.2	53 ± 4	244 ± 5	16.8 ± 0.2	-16.4 ± 0.3
6. NaF	70 ± 6	198 ± 6	-3.3 ± 0.3	3.4 ± 0.4	61 ± 7	221 ± 9	7.3 ± 0.4	-7.3 ± 0.3	52 ± 6	235 ± 5	16.4 ± 0.4	-16.4 ± 0.4
7. NaBr	81 ± 5	190 ± 9	-3.7 ± 0.4	3.8 ± 0.5	73 ± 5	200 ± 6	5.3 ± 0.3	-5.4 ± 0.3	50 ± 4	255 ± 5	16.7 ± 0.2	-16.8 ± 0.4
8. NaI					96 ± 5	176 ± 4	4.1 ± 0.3	-4.2 ± 0.3	66 ± 4	238 ± 6	16.0 ± 0.2	-16.4 ± 0.3
9. $NaClO_4$	77 ± 5	194 ± 7	-3.5 ± 0.2	3.1 ± 0.2								
10. NaAc[a]	78 ± 5	196 ± 8	-3.6 ± 0.3	3.6 ± 0.4	55 ± 6	214 ± 7	7.4 ± 0.3	-7.3 ± 0.4	72 ± 5	229 ± 7	15.3 ± 0.4	-16.2 ± 0.5
11. CsAc[a]									84 ± 5	226 ± 5	14.1 ± 0.4	-14.3 ± 0.3
12. NH_4I									70 ± 8	228 ± 9	15.8 ± 0.4	-15.6 ± 0.5
13. none[b]	80 ± 3	196 ± 5	-3.6 ± 0.3	3.4 ± 0.4	84 ± 6	185 ± 8	5.2 ± 0.3	-5.5 ± 0.2	72 ± 3	228 ± 2	14.9 ± 0.2	-15.2 ± 0.2

[a] Ac = $CH_3CO_2^-$. [b] For $Ru(bpy)(CN)_4^{2-}$ the data in water were taken from ref 1.

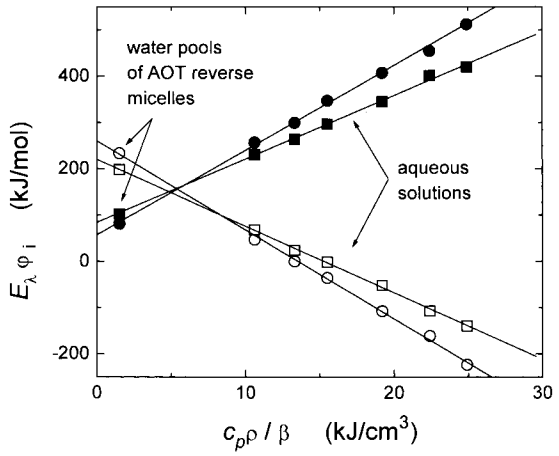

Figure 4. $E_\lambda\varphi_1$ and $E_\lambda\varphi_2$ values associated with the formation (filled symbols) and decay (open symbols), respectively, of the ^{3}MLCT state of $Ru(bpy)(CN)_4^{2-}$ vs ($c_p\rho/\beta$) of the medium, in (squares) 0.1 M CsCl solutions and in (circles) 0.1 M $N(CH_3)_4Cl$ solutions, together with the $E_\lambda\varphi_i$ values obtained in AOT/*n*-heptane/$R = 20$ reverse micelles dispersions at 25 °C. The temperatures for the measurements in aqueous solutions were from left to right 40, 30, 25, 20, 17, and 15 °C.

this term is neglected since it is within the experimental uncertainties of the values. Taking into account that the quantum yields of formation and decay of the ^{3}MLCT states are unity, i.e., $\Phi_1 = \Phi_2 = 1$, eq 3 can be rewritten as eq 4,

$$\Delta H_{str} = E_\lambda - q_1 = q_2 \tag{4}$$

where ΔH_{str} is the total heat stored upon the structural change, i.e., formation (and released upon decay), of the ^{3}MLCT state. In every case, eq 4 was fulfilled. The ΔH_{str} values resulted to be very similar when calculated either by using q_1 or q_2 (Table 1).

The slopes of the lines such as shown in Figure 4, ΔV_1 and ΔV_2, are the total structural volume changes associated with each of these two processes, respectively. Again, since $\Phi_1 = \Phi_2 = 1$, those slopes directly yield the molar structural volume change $\Delta V_{str,1}$ for the formation and $\Delta V_{str,2}$ for the decay of the complex in the various salt solutions (Table 1) and fulfill the volume balance equation $\Delta V_{str,1} = -\Delta V_{str,2}$.

This result was expected since the ^{3}MLCT states fully return to the ground state of the respective complex, as evidenced by the fact that $(\varphi_1 + \varphi_2) = 1$ in every case.

The data with $Ru(bpy)(CN)_4^{2-}$ in AOT micelles with 0.1 M salt solutions in the water pools (shown in Figure 4 for the two salts depicted) were used in order to expand the ($c_p\rho/\beta$) range and decrease the error of the derived parameters, in particular those of the intercepts, i.e., of the values of the heat evolved.[2] However, this approach could not be applied with the neutral $Ru(bpy)_2(CN)_2$ complex, since partition effects could arise and therefore its location in the center of the water pools was not warranted. Neither could the approach of including the complex into a reverse micelle be used with $Ru(bpy)_3^{2+}$, since it is known that this complex remains bound to the anionic interface of AOT,[15] where the microenvironment differs from bulk water even at large R values.[16]

For the subsequent calculations, the averages of the experimental values for each salt (Table 1) were used, i.e., $\Delta H_{str} = [(E_\lambda - q_1) + q_2]/2$ and $\Delta V_{str} = (\Delta V_1 - \Delta V_2)/2$. For both ruthenium cyano complexes, the variation in the ΔV_{str} and ΔH_{str} values with respect to the values in water is much larger than the experimental error of the measurements. This is not the case for $Ru(bpy)_3^{2+}$.

Discussion

As already discussed in our previous publications[1,2,10] and outlined above, in each case the amplitude of the first component of the deconvolution fitting function, φ_1, is associated with the formation of the ^{3}MLCT state of the respective complex, whereas the second component represents the decay of this state with lifetime τ_2 (Scheme 1).

The magnitude and sign of ΔV_i depend on the complex. Upon formation of the ^{3}MLCT state of $Ru(bpy)_3^{2+}$, a contraction is observed, instead of the expansions observed for the cyano complexes. This is understood in terms of different origins of the structural volume changes for these complexes.

The structural volume changes of the Ru(II) cyano complexes originate in the photoinduced changes in the hydrogen bond interaction between the cyanide ligands and the water molecules.[1,2] For $Ru(bpy)_3^{2+}$, on the contrary, the contraction has been attributed to a shortening of the Ru−bpy bond upon ^{3}MLCT formation.[17] Therefore, as expected, for $Ru(bpy)_2(CN)_2$ and $Ru(bpy)(CN)_4^{2-}$, the values of ΔV_{str} and of ΔH_{str} depend on the nature of the salt solutions, whereas for $Ru(bpy)_3^{2+}$ they do not.

For the cyano complexes there is a linear correlation between the values of ΔH_{str} and ΔV_{str} along the salt series (Figure 5).

The variation in the values of ΔV_{str} and of ΔH_{str} with the nature of the salt cannot be attributed to specific interactions of the salts with the complexes, since no changes in the

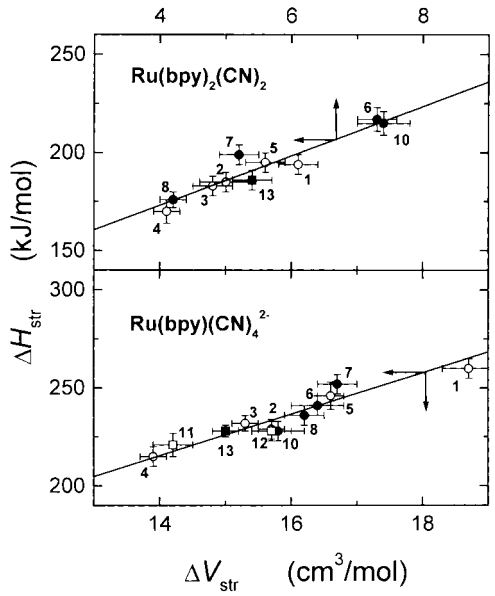

Figure 5. Total enthalpy change determined by LIOAS upon formation of the respective ^{3}MLCT state, ΔH_{str}, vs the structural volume change, ΔV_{str}, for $Ru(bpy)_2(CN)_2$ (upper panel) and $Ru(bpy)(CN)_4^{2-}$ (lower panel). Numbers follow the order in Table 1 with (○) chloride salts (1−5), (●) sodium salts (5−10), (□) CsAc (11), and NH_4I (12). Solid lines are linear regressions of the data, $r = 0.945$ and 0.937 for $Ru(bpy)_2(CN)_2$ and for $Ru(bpy)(CN)_4^{2-}$, respectively. In each case $\Delta H_{str} = [(E_\lambda - q_1) + q_2]/2$ and $\Delta V_{str} = [\Delta V_1 - \Delta V_2]/2$ (Table 1).

SCHEME 1: Term Scheme Showing the Processes Taking Place upon Excitation and Decay of the Cyano Complexes Studied in This Work (ΔH_{str} > or < E_{MLCT}, Depending on the Salt Present)

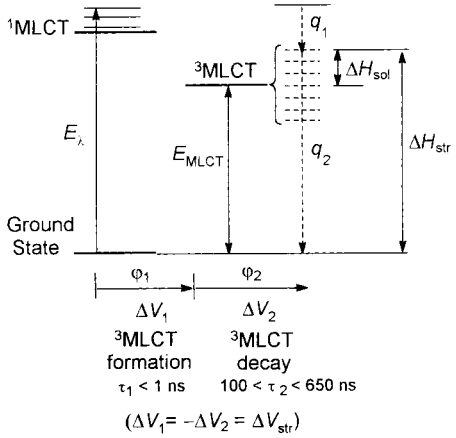

spectroscopic properties of the complexes were observed. Thus, the added electrolytes affect neither the ground state nor the ^{3}MLCT state energy level (as detected optically) of the complexes. The constancy of the ^{3}MLCT complexes lifetimes in water and in salt solutions demonstrates that dynamic quenching processes do not occur either. Therefore, the differences in the structural volume changes and in the heat evolved in the presence of the various salts should be assigned to changes in the environment induced by the electrolytes.

Structural Enthalpy−Volume Correlation. Equation 5 depicts the empirical linear correlation between ΔH_{str} and ΔV_{str} for both cyano complexes in the presence of the various salts (Figure 5).

$$\Delta H_{str} = C + X\Delta V_{str} \tag{5}$$

Linear regression of the data affords the intercept and slope values of (123 ± 8) kJ/mol and (12.6 ± 1.5) kJ/cm^3 for $Ru(bpy)_2(CN)_2$, and of (67 ± 25) kJ/mol and (10.6 ± 1.6) kJ/cm^3 for $Ru(bpy)(CN)_4^{2-}$.

The values of the structural enthalpy change, ΔH_{str}, as well as those of the structural volume change, ΔV_{str}, and the structural entropy change, ΔS_{str}, contain additive contributions due to intrinsic ($\Delta Y_{int} = \Delta Y_{MLCT}$) and solvent ($\Delta Y_{sol}$) changes (eq 6, with $Y = H$, V, or S).

$$\Delta Y_{str} = \Delta Y_{MLCT} + \Delta Y_{sol} \tag{6}$$

The additivity of intrinsic and environmental contributions to thermodynamic parameters has been used successfully in the past and reflects the fact that both contributions are considered independent of each other.[9,18] The intrinsic contributions obviously include the changes induced in the hydrogen bound water molecules to the CN groups. Equation 5, rewritten in terms of the separate contributions turns into eq 7

$$\Delta H_{MLCT} + \Delta H_{sol} = C + X[\Delta V_{MLCT} + \Delta V_{sol}] \tag{7}$$

Since the energy levels of the MLCT state (singlet and triplet) are not changed by the addition of salts (see Figure 1), $\Delta H_{MLCT} = E_{MLCT}$ should be constant for each complex along the salt series. The value of ΔV_{MLCT} (mainly changes in bond lengths, including those of the CN- - -HOH bonds) due to the photooxidation of Ru(II) to Ru(III) upon formation of the ^{3}MLCT state should also be independent of the salt for each complex.

Therefore eqs 7 and 8 can be used, e.g., to calculate the perturbation ($\delta\Delta Y$, with $Y = V_{str}$ or H_{str}) induced by the salts

$$\delta\Delta Y_{str} = \Delta Y_{str,salt} - \Delta Y_{str,w} \tag{8}$$

(salt) with respect to the values in neat water (w). The perturbation of the structural volume change induced by the salt with respect to the value in neat water ($\delta\Delta V_{str}$) obviously also linearly correlates with the perturbation of ΔH_{str} ($\delta\Delta H_{str}$) (figure not shown).

Should $\delta\Delta H_{str}$ (eq 8) be the result of a change in the ^{3}MLCT energy level, a ca. 100 nm shift would have been observed between the emission maximum for $Ru(bpy)(CN)_4^{2-}$ in 0.1 M $N(CH_3)_4Cl$ and in 0.1 M CsCl solutions. This is certainly much larger than the experimental error of the spectral measurements.

The linearity of the plots in Figure 5 confirms that the perturbations are only due to environmental effects and that the intrinsic heat and structural volume changes are constant for each complex along the salt series.

Contrary to the values of ΔH, ΔV, and ΔS, the value of the free energy associated with the formation of the ^{3}MLCT state of the respective cyano complex ΔG_{MLCT} (including the free energy involved in the changes of the CN- - -HOH bonds) does not depend on the environment reorganization, i.e., $\Delta G_{sol} = 0$.[9] Thus, the general eq 9 is written

$$\Delta H_{str} = \Delta G_{MLCT} + T\Delta S_{str} = \Delta G_{str} + T\Delta S_{str} \tag{9}$$

With this equation and the empirical correlation (5), eq 10 is readily obtained:

$$C + X\Delta V_{str} = \Delta G_{MLCT} + T\Delta S_{str} \tag{10}$$

The plots in Figure 5 in fact reflect eq 10, i.e., there is an empirical linear correlation with the form $\Delta S_{str} = (X/T)\Delta V_{str}$. The values of ΔV_{str} are thus associated with entropy changes related to the ability of the added salts to interfere with the hydrogen-bond network of water. Entropy−volume correlations in water have been observed for several reactions, such as the

ionization of acids,[19] the protonation of amines,[20] the hydration changes in DNA−ligand interactions,[21] and the formation of nucleic acid homoduplexes in different conformations.[22] The volume−entropy relationship has been the object of detailed analysis, especially for reactions in hydrogen-bonding solvents.[23] The large decrease in ΔV_{str} for $Ru(bpy)(CN)_4^{2-}$ when incorporated in a AOT reverse micelle with a small value of $R = [H_2O]/[AOT]$ confirms the linear correlation between ΔV_{str} and the entropy change, since high rigidity as encountered in the inner pool of a micelle with small R should strongly reduce the entropy change upon formation of the ^{3}MLCT state.[2]

Enthalpy−Entropy Compensation. The slopes of the plots ΔH_{str} vs ΔV_{str} for both $Ru(bpy)_2(CN)_2$ and $Ru(bpy)(CN)_4^{2-}$ (Figure 5) were perfectly linear and yielded similar slopes within error limits; i.e., in eq 10, $X = (12.6 \pm 1.5)$ kJ/cm^3 for $Ru(bpy)_2(CN)_2$ and (10.6 ± 1.1) kJ/cm^3 for $Ru(bpy)(CN)_4^{2-}$, indicating that in both cases the same effect is operating. The value of X is very similar to the ratio of thermoelastic parameters ($c_p\ \rho/\beta$) in 0.1 M salt solutions at a temperature between 30 and 40 °C (see section on LIOAS signal handling). Since we have empirically shown that the structural volume change is a measure of the entropy change, the linearity of the plots in Figures 5 reflects an enthalpy−entropy compensation effect upon perturbation of the environment by the salt.

The enthalpy−entropy compensation effect arises in dilute solutions, e.g., when several molecular species are in dynamic equilibrium in solution and this equilibrium is perturbed by a particular factor, such as the addition of salts in the present case. Since water molecules have strong tendency to participate as both hydrogen bond donors and acceptors, the favorable formation of hydrogen bonds between the same added solute and the water molecules should produce a decrease in enthalpy. In turn, hydrogen bonds require that the participating molecules become relatively fixed; therefore, the entropy also decreases.[9] Thus, taking into account that a hydrogen bond implies ca. 17 kJ/mol,[24,25a] for the salts at the extremes of the plots in Figure 5, a difference of ca. 2−3 hydrogen bonds in excess or defect with respect to neat water are perturbed upon excitation.

In general, it is difficult to detect these enthalpy−entropy compensation effects especially since the magnitude of the environmental effect might be much smaller than the intrinsic or nominal effect. In some cases, the variation may be masked by statistical compensations arising from experimental errors.[26] This is particularly so for the activation parameters derived from Arrhenius plots due to the large extrapolations involved in the determination of the preexponential factor.[27,28] In our case the extrapolations are not very large, and particularly for $Ru(bpy)(CN)_4^{2-}$, the experiments inside the AOT dispersions decreased the error by 1 order of magnitude,[2] permitting us to have a large confidence in the data.

We note that along the salt series the values of $(\delta\Delta V_{str}/\Delta V_{str})$ are larger than the values of $(\delta\Delta H_{str}/\Delta H_{str})$, making the determination of the changes in structural volume changes a more sensitive probe for environmental effects.

Entropic Factor Associated with the ^{3}MLCT State Formation. The correlation between the structural volume change and the structural entropic change (eq 10, Figure 5) affords the value of the free energy for the formation of the ^{3}MLCT state, which is $C = \Delta G_{MLCT} = (123 \pm 8)$ kJ/mol for $Ru(bpy)_2(CN)_2$ and (67 ± 25) kJ/mol for $Ru(bpy)(CN)_4^{2-}$; i.e., the latter complex is much more stable than the former.

For $Ru(bpy)_2(CN)_2$, $\Delta G_{MLCT} = (123 \pm 8)$ kJ/mol together with $E_{MLCT} = 222$ kJ/mol (±10%, onset of the emission band[1]) affords the value of $T\Delta S_{MLCT} = (99 \pm 30)$ kJ/mol. For $Ru(bpy)(CN)_4^{2-}$, $\Delta G_{MLCT} = (67 \pm 25)$ kJ/mol together with a slightly higher value of $E_{MLCT} = 230$ kJ/mol (±10%[1]) yields a larger value of $T\Delta S_{MLCT} = (163 \pm 45)$ kJ/mol. We interpret this larger entropic factor stabilizing the complex bearing four CN groups as a result of a larger movement in the ^{3}MLCT state of $Ru(bpy)(CN)_4^{2-}$ due to the loosening of a larger number of CN- - -HOH bonds upon photoexcitation, i.e., four instead of two in $Ru(bpy)_2(CN)_2$.

Structural Volume Changes vs Water-Structuring Entropy Changes. It is well documented that the random hydrogen-bound water network continually undergoes rearrangement, with bonds being strained, broken, and then reformed.[9,25] Roughly half of the potential hydrogen bonds are present at any instant. The value of the entropy change due to the effect of the ions on the structure of the water, $\Delta S°_{str}$, for the individual ions has been calculated by Marcus[29,30] by subtracting from the standard entropy of hydration nonstructural sources such as electrostatic interactions, changes of volume between standard states, the inmobilization of water molecules, and hindered rotations in polyatomic ions.[31] Thus, the quantity $\Delta S°_{str}$ is regarded as proportional to the ability of the ions to modify the equilibrium in this "normal" three-dimensional network, disrupting or extending the network. $\Delta S°_{str}$ is negative for structure-making and positive for structure-breaking ions.

We find that ΔV_{str} for the Ru(II) cyano complexes can be correlated with the entropy change introduced by the salts on the network structure of water, $\Delta S°_{str}(salt)$, calculated as the sum of the contribution of the individual ions,[30] eq 11, by making the assumption that their behavior is additive and that specific interactions between them do not occur.

$$\Delta S°_{str}(salt) = \Delta S°_{str}(anion) + \Delta S°_{str}(cation) \qquad (11)$$

In the present work we used simple monovalent sodium and chloride salts. The individual $\Delta S°_{str}$ values for Na^+ and Cl^- are −16 and +12 J/K mol, respectively. Thus, NaCl should not produce any important change on the hydrogen-bond network of water, since its calculated $\Delta S°_{str}(salt)$ is close to zero. The same can be assumed for salts with $\Delta S°_{str}(salt)$ within the value ±20 J/K mol, since, due to some uncertainties in the estimation of this parameter, ions with $\Delta S°_{str}$ values between −20 and +20 J/K mol may afford unreliable assignments.[30,31] Within this framework, salts with values of $\Delta S°_{str}(salt)$ 20 J/K mol more negative than $\Delta S°_{str}(NaCl)$ such as NaF, NaAc (Ac = acetate), and $N(CH_3)_4Cl$ are structure-making salts, whereas CsCl, NaI, and NH_4I are structure-breaking salts, with $\Delta S°_{str}(salt)$ values 20 J/K mol more positive than $\Delta S°_{str}(NaCl)$.

The slope of ΔV_{str} vs $\Delta S°_{str}(salt)$ depends on the complex (Figure 6). For $Ru(bpy)_3^{2+}$, the ΔV_{str} values are constant, since this complex is unable to interact with water through the bipyridine hydrophobic ligands. As expected, no effect of the salts on ΔV_{str} for this complex is found since the value of ΔV_{str} is mainly determined by internal rearrangements.[17]

A striking good correlation is observed for the neutral $Ru(bpy)_2(CN)_2$ complex, whatever the nature of the salt is (sodium or chloride series). ΔV_{str} increases as the structure-making properties of the salts increase, i.e., for more negative $\Delta S°_{str}(salt)$ values (Figure 6).

This correlation supports our interpretation in terms of the ion-induced perturbation of the hydrogen-bond equilibria in the water network.[9] Upon photoinduced formation of the ^{3}MLCT state of the Ru(II) cyano complexes a larger expansion in the presence of structure-making, i.e., a more negative value of $\Delta S°_{str}(salt)$, is then explained by the formation of a larger

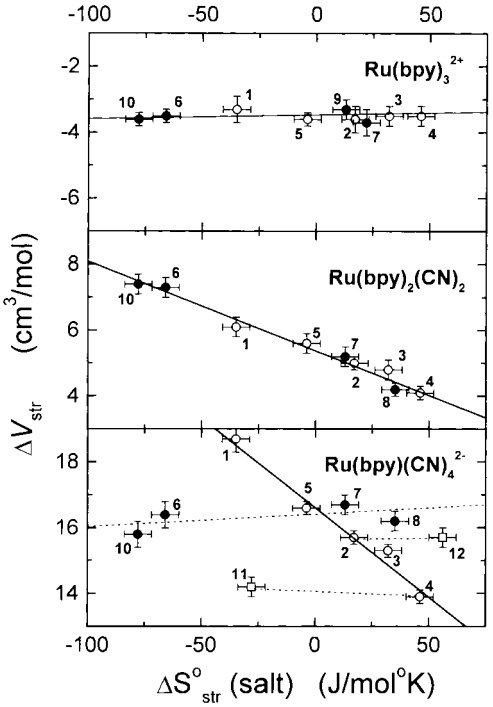

Figure 6. Structural volume changes, ΔV_{str}, associated with the ^{3}MLCT state formation of $Ru(bpy)_3^{2+}$, $Ru(bpy)_2(CN)_2$, and $Ru(bpy)(CN)_4^{2-}$ as a function of the structural standard entropy changes of the salts, $\Delta S°_{str}$(salt), calculated (eq 8) with the values of the individual ions as reported.[30] Numbers follow the order in Table 1 with (○) chloride salts (1−5), (●) sodium salts (5−10), (□) CsAc (11), and NH_4I (12). Solid lines are linear regressions of the data, $r = 0.992$ and 0.977 for $Ru(bpy)_2(CN)_2$ and for $Ru(bpy)(CN)_4^{2-}$, respectively. For $Ru(bpy)(CN)_4^{2-}$ the dotted lines are linear regressions of the data for the same cation and variable anions.

number of hydrogen bonds (a more extended hydrogen-bond network) associated with the solvation sphere of the complex. In the presence of structure-breaking salts, i.e., a more positive $\Delta S°_{str}$(salt) value, the situation should be the opposite, with a less extended hydrogen-bond network and a smaller expansion.

For $Ru(bpy)(CN)_4^{2-}$ in chloride salt solutions, ΔV_{str} also correlates with $\Delta S°_{str}$ (open circles in Figure 6). In the sodium series, however, ΔV_{str} experiences only a very slight change with the variation of the anionic counterion (filled circles in Figure 6). Similarly, almost identical ΔV_{str} values are determined in CsAc and in CsCl solutions, as well as in NH_4I and in NH_4Cl solutions (open squares in Figure 6).

The rationale for this behavior lies in the fact that, for the anionic complex, some ion pairing with the cations should occur, although this ion pairing (probably a solvent-separated pair) obviously does not modify the electronic properties as evidenced by the invariance of the absorption spectra.[32] On the basis of the calculation by Clark and Hoffman for $Ru(bpy)_3^{2+}$,[33] and taking into account that both complexes have the same number of charges and a similar radius, we estimate that under our experimental conditions $Ru(bpy)(CN)_4^{2-}$ is largely paired with at least one cation.

Thus, Cs^+, K^+, Na^+, NH_4^+, and $N(CH_3)_4^+$ modify the network structure of the water molecules solvating the complex, without interacting directly with the CN groups, and a dependence of ΔV_{str} with $\Delta S°_{str}$(salt) is obtained. On the other hand, variation of the anion for the same cation has a much smaller effect since anions are shielded from the negatively charged complex by the local effect of the ion pairing. Contrary to the cations, protons do replace the water molecules bound to the CN groups in $Ru(bpy)(CN)_4^{2-}$, leading to strong pH-dependent changes in the absorption spectra[6] and in the structural volume changes.[34]

The ion pairing also expected to occur with $Ru(bpy)_3^{2+}$ is irrelevant for the structural volume change observed with this complex, since the change is only determined by internal rearrangement (vide supra). Since $Ru(bpy)_2(CN)_2$ is a neutral complex, ion pairing does not take place and ΔV_{str} linearly depends on $\Delta S°_{str}$(salt), regardless of the nature of the salt (Figure 6).

The slope $\Delta V_{str}/\Delta S°_{str}$ for $Ru(bpy)(CN)_4^{2-}$ is practically twice as large as that observed for $Ru(bpy)_2(CN)_2$. This result is in agreement with previous data showing a dependence on the number of the cyano groups of parameters such as redox potentials, ionization energies, spectra maxima,[3,4] and structural volume changes for the formation of the ^{3}MLCT states of Ru(II) cyano complexes,[1] supporting the hypothesis that the change in specific interaction of water with the cyano ligands upon ^{3}MLCT state formation is the origin of the effect and that the influence at each perturbed cyanide is additive. In particular, the values ΔV_{str} correlate relatively well with the number of CN ligands perturbed by the excitation, as long as the lowest state is purely a MLCT state. Thus, in neat water, ca. 15 cm^3/mol is measured for $Ru(bpy)(CN)_4^{2-}$, 10 cm^3/mol for $Ru(bpy)(CNCH_3)(CN)_3^-$, and 5 cm^3/mol for $Ru(bpy)_2(CN)_2$.[1] It is possible to conjecture that the value 0 cm^3/mol observed for $Ru(bpy)(CN)_2(CNCH_3)_2$ arises from the mixing of LC and MLCT character in the lowest excited level of this compound[3b] since the expected value $\Delta V_{str} = 0$ was measured for the complex $Ru(CN)(CNCH_3)_3^+$ for which it is established that the lowest excited state has an LC character.[1]

Conclusions

For the Ru(II) cyano complexes, the photoinduced structural volume changes correlate, on one side, with the change in structural entropy induced by an added salt and, on the other side, with the heat evolved during the same process. The magnitude of these parameters depends on the more or less ordered structure of the hydrogen-bond network in the water, since the bonds CN- - -HOH in these complexes are very sensitive to this order and are weakened upon photooxidation of the metal center. For $Ru(bpy)_3^{2+}$ the effect is not observed, since it has no ligands specifically bonding water.

The above-mentioned effect of the added salts on the photoinduced heat and structural volume changes is interpreted as an enthalpy−entropy compensation effect due to reorganization of the environment (water) surrounding the photoinduced species.

Small changes introduced by the salts in the equilibrium between the various molecular species in water are at the basis of the enthalpy−entropy compensation effect. For a more organized water structure, the value of ΔV_{str} is larger since the effect comprises a more extended network and the corresponding evolved heat becomes larger due to the larger number of hydrogen bonds involved. Smaller ΔV_{str} values and less heat evolution accompany ^{3}MLCT formation in a less organized water structure. The larger expansion observed for salts showing a more negative calculated $\Delta S°_{str}$(salt) value (structure making salts) is thus explained by the extension of the hydrogen-bond network, whereas the smaller expansion for salts with a more positive $\Delta S°_{str}$(salt) value should be due to a smaller network.

The enthalpy−entropy compensation effect permits the determination of the free energy associated with the ^{3}MLCT formation, which at room temperature is largely determined by

the entropic factor $T\Delta S_{MLCT}$. For the two cyano compounds studied, $T\Delta S_{MLCT}$ is related to the number of water-bound CN groups, i.e., the compound with four of those groups has a larger flexibility in its ^{3}MLCT state, since four hydrogen bonds to water molecules become loosened upon photoexcitation, rather than two in the molecule with two CN groups bound to water.

The finding that the heat evolved also depends on the chromophore−solvent interaction (especially in water) has far reaching implications for the interpretation of calorimetric data obtained by LIOAS and by other photothermal methods. The photothermal value should not necessarily coincide with the energy content derived from optical methods. Photocalorimetric data may contain contributions from the photoinduced changes in the environment (see Scheme 1). This is particularly so for solutes bearing substituents which form strong bonds with the solvent such as, e.g., hydrogen bonds with water. In the cyano complexes, ca. 10−20% (depending on the salt) of the heat evolved is due to changes in the solvent upon photoproduction of the transient species. Thus, the difference between the energy values obtained by photothermal methods and those derived from optical methods may afford the time-resolved solvent reorganization enthalpy in a photoinduced reaction producing transient species.

On the contrary, the heat evolved upon excitation of Ru(bpy)$_3^{2+}$ reflects more accurately the energy content of the ^{3}MLCT state, since no specific interactions with water are expected with this compound.

For the intramolecular electron-transfer reaction studied in the present work, $\Delta S_{str} = (X/T)\Delta V_{str}$, with X very similar to the ratio of thermoelastic parameters ($c_p\rho/\beta$) of the medium at a temperature within the analyzed range. This realization opens the possibility of determining the entropy changes for the photoinduced formation of transient species by using the structural volume changes measured by photothermal methods.

Acknowledgment. We are indebted to Professor Kurt Schaffner for his continuous support. The technical help from Dagmar Lenk, Gudrun Klimm, and Sigrid Russell is greatly appreciated. Discussions with Dr. Enrique San Román (Buenos Aires) were very helpful. We are very grateful to Professor Ernest Grunwald (Brandeis University) for making clear several concepts to us.

References and Notes

(1) Habib Jiwan, J.-L.; Wegewijs, B.; Indelli, M. T.; Scandola, F.; Braslavsky, S. E. *Recl. Trav. Chim. Pays-Bas*. **1995**, *114*, 542−548.

(2) Borsarelli, C. D.; Braslavsky, S. E. *J. Phys. Chem. B* **1997**, *101*, 6036−6042.

(3) (a) Bignozzi, C. A.; Chiorboli, C.; Indelli, M. T.; Rampi Scandola, M. A.; Varani G.; Scandola, F. *J. Am. Chem. Soc.* **1986**, *108*, 7872−7873. (b) Scandola, F.; Indelli, M. T. *Pure Appl. Chem.* **1988**, *60*, 973−980.

(4) Timpson, C. J.; Bignozzi, C. A.; Sullivan, B. P.; Kober, E. M.; Meyer, T. J. *J. Phys.* Chem. **1996**, *100*, 2915−2925.

(5) García Posse, M. E.; Katz, N. E.; Baraldo, L. M.; Polonuer, D. D.; Colombano, C. G.; Olabe, J. A. *Inorg. Chem.* **1995**, *34*, 1830−1835.

(6) Indelli, M. T.; Bignozzi, T. A.; Marconi, A. M.; Scandola, F. In *Photochemistry and* Photophysics of Coordination Compounds; Yersin, H., Vogler, A., Eds.; Springler-Verlag: Berlin, 1987; p 159.

(7) Balzani, V.; Sabbatini N.; Scandola, F. *Chem. Rev.* **1986**, *86*, 319−337.

(8) (a) Peterson, S. H.; Demas, J. N. *J. Am. Chem. Soc.* **1976**, *98*, 7880−7881. (b) Peterson, S. H.; Demas, J. N. *J. Am. Chem. Soc*. **1979**, *101*, 6571−6577.

(9) (a) Grunwald, E.; Comeford, L. L. In *Protein−Solvent Interactions*, Gregory, R. B., Ed.; Marcel Dekker: New York, 1995; Chapter 10. (b) Grunwald, E. *Thermodynamics of Molecular Species*; Wiley: New York, 1997.

(10) Borsarelli, C. D.; Corti, H.; Goldfarb, D.; Braslavsky, S. E. *J. Phys. Chem. A* **1997**, *101*, 7718−7724.

(11) Hildenbrand, K.; Nicolau, C. *Biochim. Biophys. Acta* **1979**, *553*, 365−377.

(12) Habib Jiwan, J.-L.; Chibisov, A. K.; Braslavsky, S. E. *J. Phys. Chem.* **1995**, *99*, 10246−10250.

(13) Weast, R. C., Ed. *CRC Handbook of Chemistry and Physics*, 67th ed.; CRC Press: Boca Raton, FL, 1986−87; pp F-4, F-5.

(14) Juris, A.; Balzani, V.; Barigelletti, F.; Campagna, S.; Belser, P.; von Zelewsky, A. *Coord. Chem. Rev.* **1988**, *84*, 85−277 and references therein.

(15) Jada, A.; Lang, J.; Zana, R. *J. Phys. Chem.* **1990**, *94*, 387−395.

(16) See for example: (a) Luisi, P. L., Straub, B. E., Eds. *Reverse Micelles*; Plenum Press: New York, 1984. (b) Pileni, M. P., Ed. *Structure and Reactivity in Reverse Micelles*; Elsevier: Amsterdam, 1989.

(17) Goodman, J. L.; Herman, M. S. *Chem. Phys. Lett.* **1989**, *163*, 417−420.

(18) Pollmann, P.; Rehm, D.; Weller, A. *Ber. Bunsen-Ges. Phys. Chem.* **1975**, *79*, 692−696.

(19) Hepler, L. G. *J. Phys. Chem.* **1965**, *69*, 965−967.

(20) Cabani, S.; Mollica, V.; Lepori, L.; Lobo, S. T. *J. Phys. Chem.* **1977**, *81*, 987−993.

(21) Rentzeperis, D.; Marky, L. A.; Kupke, D. W. *J. Phys. Chem.* **1992**, *96*, 9612−9613.

(22) Rentzeperis, D.; Kupke, D. W.; Marky, L. A. *Biopolymers* **1993**, *33*, 117−125.

(23) Phillips, J. C. *J. Phys. Chem.* **1985**, *89*, 3060−3066.

(24) Feyereisen, M. W.; Feller, D.; Dixon, D. A. *J. Phys. Chem.* **1996**, *100*, 2993−2997.

(25) See for example the following articles and references therein: (a) Stilliger, F. H. *Science* **1980**, *209*, 451−457. (b) Israelachvili, J.; Wennerström, H. *Nature* **1996**, *379*, 219−225. (c) Grunwald, E.; Steel, C. *J. Phys. Chem.* **1993**, *97*, 13326−13329.

(26) Krug, R. R.; Hunter, W. G.; Grieger, R. A. *J. Phys. Chem.* **1976**, *80*, 2335−2341.

(27) Twigg, M. V. *Inorg. Chim. Acta* **1977**, *24*, L84−L86.

(28) Lawrence, G. A.; Suvachittanont, S. *Inorg. Chim. Acta* **1979**, *32*, L13−L15.

(29) Marcus, Y. *J. Chem. Soc., Faraday Trans. 1* **1986**, *82*, 233−242.

(30) Marcus, Y. *Ion Solvation*; John Wiley: New York, 1985. The ΔS_{str} values for the individual ions used in eq 2 were extracted from Table 5.13, p 125, of this publication.

(31) Marcus, Y. *Biophys. Chem.* **1994**, *51*, 111.

(32) Billing, R.; Rehorek, D.; Hennig, H. *Top. Curr. Chem.* **1990**, *158*, 151−158.

(33) Clark, C. D.; Hoffman, M. Z. *J. Phys. Chem.* **1996**, *100*, 7526−7532.

(34) Borsarelli, C.; Braslavsky, S. E. *J. Photochem. Photobiol. B: Biol.* **1998**, in press.